ANNALS OF GEOPHYSICS, 66, 6, SE641, 2023; doi.10.4401/ag-8938
OPEN ACCESS

Double resonance in seismo-lithosphere-atmosphere-ionosphere coupling

Chieh-Hung Chen[*,1], Yang-Yi Sun[1], Xuemin Zhang[2], Yongxin Gao[3], Aisa Yisimayili[4], Haiyin Qing[5], Ta-Kang Yeh[6], Kai Lin[1], Fei Wang[7], Horng-Yuan Yen[8], Cheng-Horng Lin[9], Jann-Yenq Liu[10,11,12]

(1) Institute of Geophysics and Geomatics, China University of Geosciences, Wuhan 430074, China
(2) Institute of Earthquake Forecasting, China Earthquake Administration, Beijing 100036, China
(3) Institute of Applied Mechanics, School of Civil Engineering, Hefei University of Technology, Hefei, 230009, China
(4) Earthquake Agency of Xinjiang Uygur Autonomous Region, Urumqi, Xinjiang, 830011, China
(5) School of Electronic Information and Artificial Intelligence, Leshan Normal University, 614000, China
(6) Department of Real Estate and Built Environment, National Taipei University, New Taipei, 10478, Taiwan
(7) Chengdu University of Technology, Chengdu 610059, China
(8) Department of Earth Sciences, National Central University, Taoyuan, 320317, Taiwan
(9) Institute of Earth Sciences, Academia Sinica, Taipei, 11529, Taiwan
(10) Department of Space Science and Engineering, National Central University, Taoyuan, 320317, Taiwan
(11) Center for Space and Remote Sensing Research, National Central University, Taoyuan, 320317, Taiwan
(12) Center for Astronautical Physics and Engineering, National Central University, Taoyuan, 320317, Taiwan

Article history: received January 21, 2023; accepted July 11, 2023

Abstract

Investigations into causal mechanisms behind anomalous pre-earthquake phenomena are considered a promising way of earthquake prediction. Numerous promising channels for seismo-lithosphere-atmosphere-ionosphere coupling have been proposed; however, predicting earthquakes remains a great challenge in the scientific society. Short-period ground vibrations exhibiting frequency characteristics similar to natural frequencies caused by strata failure resonance have recently been detected using tiltmeters embedded in magnetometers prior to earthquakes. These vibrations originate from regions near the epicentres of forthcoming earthquakes and can be simultaneously detected by broadband seismometers and ground-based global navigation satellite system (GNSS) receivers. Unlike the total electron contents (TECs) obtained from orbiting satellites, the vibrations and the identifiable TEC perturbations in data from geostationary satellites of the BeiDou Navigation System share frequencies prior to earthquakes. However, the causal relationship between the vibrations and TEC perturbations remains unclear due to a gap in data observations between the lithosphere and ionosphere. To address this issue, an instrumental array was established to monitor vibrations and perturbations in the lithosphere, atmosphere, and ionosphere. Observational data from the array partially fill the gap, and analytical results show that ground vibrations, air pressure, magnetic fields, and TEC data shared a common frequency of approximately 5×10^{-3} Hz (5 mHz) before major earthquakes. This suggests that the resonant ground vibrations trigger atmospheric resonance before earthquakes. Therefore, the double resonance (crustal and atmospheric resonance) model is a new explanation for the observed anomalies in multiple geophysical parameters in the lithosphere, atmosphere, and ionosphere. Retrieving resonant signals from multiple sources of observational data is a significant challenge, but once this issue is overcome, double resonance may contribute to practical earthquake prediction.

Keywords: Lithosphere; Atmosphere and Ionosphere (LAI) coupling; Crustal resonance; Atmospheric resonance; Double resonance; System for Monitoring Vibrations and Perturbations in the Lithosphere; Atmosphere and Ionosphere (MVP-LAI)

1. Introduction

Earthquake prediction remains a significant scientific challenge. Investigations into anomalous pre-earthquake phenomena are considered a promising method to address this challenge [Scholz et al., 1973; Astafyeva et al., 2013; Hayakawa, 2015; Ma, 2016; Ouzounov et al., 2018]. It can be difficult to differentiate anomalous earthquake-related phenomena from recorded data. Statistical tests have therefore been employed to examine the relationships between earthquakes and several geophysical parameters [Hattori et al., 2013; Liu et al., 2013, 2016; Han et al., 2014, 2017; Chen, Huang et al., 2015; Hattori and Han, 2018; Chen, Wang et al., 2020; Zhuang et al., 2021]. Seismo-ionospheric anomalies are statistically distinct from geophysical data, such that they are considered promising candidates in earthquake prediction [Liu et al., 1996; Hayakawa, 2007], but are not yet applied in practice. Failure to predict earthquake occurrence can result in damage to the social economy.

Physical coupling has been investigated between the lithosphere, atmosphere, and ionosphere (LAI) [Sorokin et al., 2006; Pulinets and Ouzounov, 2011; Hayakawa et al., 2021a, 2022; Liu et al., 2022]. As for seismo-LAI coupling, they consider chemical, conductivity, acoustic-gravity, and electromagnetic precursors to earthquake activity [Hayakawa 2015, 2016]:

1) *Chemical*: Earthquake-related stress gradually accumulates in the crust, resulting in crack propagation prior to an earthquake [Zhuang et al., 2021]. Gases stored in the strata can then travel to the surface through these cracks. The near-surface air composition is changed by the subsurface release of gases. Variations in air composition can affect the near-surface electric field [Hao, 1989; Bleier et al., 2009; Chen, Li et al., 2022], which further drive changes in the ionosphere [Pulinets and Boyarchuk, 2004; Yasuoka et al., 2006].

2) *Conductivity*: Cracks also increase subsurface fluid migration. Increases in cloud-to-ionosphere lighting [Rodger, 1999; Takahashi et al., 2003; Hayakawa et al., 2004] can heat the ionosphere [Inan et al., 1991; Pasko et al., 1997] because of changes in the underlying conductivity by fluid migration [Cho and Rycroft, 1998; Harrison et al., 2010; 2014].

3) *Acoustic-gravity*: Variations in near-surface temperature can generate acoustic-gravity waves [VanZandt, 1985; Davies, 1990; Tsuda et al., 1994; De la Torre et al., 1999; Hickey et al., 2001; Yang and Hayakawa, 2020]. Seismo-thermal anomalies are frequently observed before major earthquakes [Tronin, 1999; Tramutoli et al., 2005, 2013; Pulinets et al., 2006; Ouzounov et al., 2006, 2007; Choudhury et al., 2006] and are considered to be a major factor dominating the acoustic-gravity response. Acoustic-gravity waves generated by seismo-thermal anomalies [Blackett et al., 2011; Qin et al., 2011; Kai, 2012; Zhang et al., 2019; Genzano et al., 2021] can propagate upward, driving changes in the total electron content (TEC) in the ionosphere [Miyaki et al., 2002; Shvets et al., 2004; Korepanov et al., 2009; Kasahara et al., 2010; Hayakawa, 2011; Sun et al., 2011].

4) *Electromagnetic*: Electromagnetic emissions are known to occur before earthquakes due to processes such as deformation and microfractures in stressed rocks [Kasahara, 1981; Hadjicontis et al., 2004]. These emissions can affect the electromagnetic field near the Earth's surface and directly interfere with the ionosphere, resulting in changes to TEC [Fraser-Smith et al., 1990; Molchanov et al., 1993, 1995; Molchanov and Hayakawa, 1995].

Although scientists have proposed these four potential channels of seismo-LAI coupling, the causal mechanisms of anomalous pre-earthquake phenomena still remain unclear. This is because multiple anomalous parameters are generally retrieved from distinct stations at different distances from the earthquake epicentre.

In 2016, an interesting phenomenon was captured by tiltmeters embedded in magnetometers in Taiwan. A magnetic array comprising five three-component fluxgate magnetometers (FRG-604RC, made in Japan) was established in Taiwan (Figure 1). Magnetometers monitor changes in the geomagnetic field routinely, sampling at a rate of 10 Hz. Tiltmeters with a sampling interval of 1 Hz were embedded in the magnetometers to determine whether the magnetic field was affected by ground tilts and/or vibrations. In general, raw tilt data exhibit diurnal and/or semi-diurnal variations due to solid tides (Figures 1a and b). On 9 April 2016, short period (~3 h) tilt data lay on diurnal and semi-diurnal variations, mainly at the NS (north-south) component at the HLG station (121.42°E, 23.59°N) (Figure 1c). In contrast, the short-period mode appeared in the EW (east-west) component at the TCD station (120.62°E, 24.33°N) (Figure 1d). The intersection between the NS direction of the HLG station and the EW direction of the TCD station is located offshore in the northeast of Taiwan. Two magnitude 5.7 earthquakes occurred close to this intersection on 11 and 27 April, 2016 (Figure 1). The period of the short-period tilt data tends to increase after the earthquakes. This observation suggests that the short-period tilt data are likely related to the earthquakes. The unusual phenomena of short-period tilts and/or ground vibrations are thus examined by utilizing two distinct instruments simultaneously.

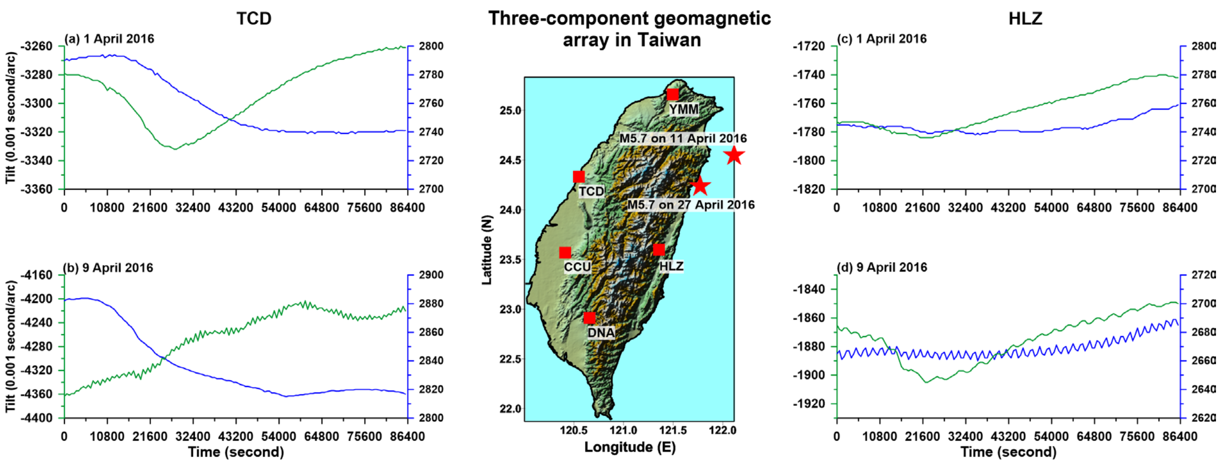

Figure 1. Variations in raw tilt data from magnetometers in Taiwan on 1 and 9 April 2016. Locations of magnetometers and related epicentres are indicated by red rectangles and red stars in the centre diagram, respectively. Station codes for each magnetometer are shown below the red rectangles. (a) and (c) show variations in tilt data on 1 April 2016 at the TCD and HLZ stations, respectively. (b) and (d) show variations in tilt data on 9 April 2016 at the TCD and HLZ stations, respectively. Blue and green lines are the NS and EW components of the tilt data, respectively.

Chen, Lin et al. [2020] collected continuous seismic data from broadband seismometers and continuous positioning data at the surface from ground-based Global Navigation Satellite System (GNSS) receivers, to examine whether short-period tilt data could be indicative of true motion and related to global earthquake occurrences. Chen, Lin et al. [2020] eliminated perturbations in the data that could be attributed to typhoons, as well as continuous ground vibration data during the 2016 M6 Meinong earthquake in Taiwan. They found that the amplitudes of seismic and GNSS data were enhanced at frequencies between 8×10^{-5} Hz and 2×10^{-4} Hz ~20 days before the earthquakes. Furthermore, the method introduced in [Tanimoto et al., 2006] was utilised to investigate the potential source locations of the ground vibrations before the earthquakes. The investigation results show that the potential source locations are located close to the epicentres. Meanwhile, the areas to which the short-period tilt data are attributed are larger than the fault rupture zones. Similar phenomena of earthquake localizations have been observed during major earthquakes in the United States, Mexico, and China [Chen, Lin et al., 2020]. This suggests that the observed ground vibrations are not a particular feature of Taiwanese earthquakes, but rather common to earthquakes worldwide.

To investigate the potential mechanism, the frequencies of ground vibrations before earthquakes are compared with the natural frequencies prior to material failure, as earthquakes are caused by fault dislocations. Chen, Lin et al. [2020] reported that the frequencies of ground vibrations roughly agreed with the natural frequencies of a square sheet, estimated using the formula proposed by Leissa [1969]. Consistent enhancements in amplitude for the ground vibrations at the same frequency band have been observed 5-10 days prior to other earthquakes. On the other hand, numerous studies have reported that earthquakes with relatively small magnitudes can be fore- and after-shocks of major events [Ellsworth and Beroza, 1995; Reasenberg, 1999; Vidale et al., 2001; Scholz, 2002]. Chen, Sun et al. [2020] re-estimated the sized of earthquake preparation zones by utilising all events from earthquake catalogues from Taiwan and Japan. They found that pre-earthquake amplitude enhancements were not limited to a particular frequency band, but tended to occur at high frequencies (up to ~0.01 Hz). Meanwhile, the enhancements with frequencies tending to high persist for more than one month before the earthquakes.

If the occurrence of ground vibrations before earthquakes is a consistent pattern, the next step is to determine how these ground vibrations change the ionosphere. Previous studies have reported that perturbations in the ionosphere can originate from typhoons [Chou et al., 2017a, 2017b], tornadoes [Nishioka et al., 2013], and ground vibrations [Liu et al., 2016a; Chen, Sun et al., 2022a] due to acoustic-gravity waves. Near-surface air pressure is an important parameter for determining whether the waves originating from ground vibrations in the lithosphere propagate upward through the atmosphere and into the ionosphere.

Chen et al. [2021a] examined air pressure data from two ground-based barometers inside and outside a cave. They found that the air inside the cave travelled outside the cave before the occurrence of the 2016 Meinong earthquake [Chen et al., 2021a]. This suggests that the air was squeezed out of the limited cave space immediately before the earthquake. The results from Chen et al. [2021a] partially support the atmospheric seismo-anomalies reported in previous studies [Dunajecka and Pulinets, 2005; Freund et al., 2022]. Ground vibrations would be another potential factor contributing to changes in TEC in the ionosphere before earthquakes by enhancing amplitude. However, the relationship between ground vibrations and changes in TEC was concluded utilizing different earthquakes and distinct instruments at a certain distance. Therefore, an array comprising distinct instruments across a given area is needed to monitor the process of perturbations and/or vibrations between the ground and space at particular altitudes to further clarify the seismo-LAI coupling.

2. The system for Monitoring Vibrations and Perturbations in LAI (MVP-LAI)

An instrumental array was established in the suburbs (29.6°N, 103.9°E) of Leshan City, Sichuan, China [Chen et al., 2021b]. The array was situated in the eastern part of the Tibetan Plateau. A local altitude difference of ~3000 m between the array and the average height of the Tibetan Plateau creates an excellent opportunity to investigate vertical wave propagation along the walls of the plateau. The instrumental array comprised 15 different instruments with 22 deceives [for more detail, please see Chen et al., 2021b; https://geostation.top]. These instruments routinely monitor variations in more than 15 geophysical parameters between the subsurface and an altitude of ~350 km. Most instruments were installed within a ~400 m^2 area to efficiently monitor vibrations and perturbations in the LAI (MVP-LAI), particularly in the vertical direction.

Following integration of observational data retrieved from the China Seismo-Electromagnetic Satellite [Shen, Zhang et al., 2018, Shen, Zhong et al., 2018] and radio occultation [Sun et al., 2016; Rajesh et al., 2021], data can be captured by the MVP-LAI system up to an altitude of ~800 km. The MVP-LAI system can be used to explore geophysical coupling via monitoring of natural hazards [Huang et al., 1985; Gufeld et al., 1992; Hayakawa et al., 1996; Molchanov and Hayakawa, 1998; Bishop and Straus, 2006; Liu et al., 2006, 2016a, 2016b; Sorokin et al., 2006, 2015; Hayakawa, 2007, 2011; Xiao et al., 2007; Oyama et al., 2008; Hayakawa and Hobara, 2010; Sun et al., 2011; Polyakova and Perevalova, 2011; Rozhnoi et al., 2013; Ryu et al., 2015; Chum et al., 2016; Kelley et al., 2017; Zhou et al., 2017; Astafyeva, 2019; Chuo et al., 2020], near-surface changes in climate [Rishbeth, 2006; Xu et al., 2008], variations in space weather [Davies, 1990], and human activities[Molchanov et al., 2001; Gokhberg et al., 1989; Chakrabarti, 2010; Laštovička and Šindelářová, 2019].

Instruments in the MVP-LAI system were selected based on numerous studies [Hayakawa, 2015, 2016, and references cited therein] to examine potential LAI coupling. Data retrieved from broadband seismometers, thermometers, and barometers were utilised to investigate potential near-surface acoustic-gravity coupling. Two broadband seismometers with a sampling rate of 100 Hz were installed at opposite corners of the study area to monitor the propagation azimuths of ground vibrations. Four thermometers and barometers were placed in wells with depths of 5, 3, and 1 m, and a thermometer screen height of ~1.5 m. The thermometers and barometers monitor changes in temperature and air pressure with a sampling interval of 2 s. A Radar Wind Profiler (RWP), a radio acoustic sounding system (RASS), and an Allsky camera were also included in the array to monitor wind fields from 0 m to ~4000 m in altitude, temperatures from 0 m to ~1000 m in altitude, and cloud shapes, respectively. The instruments aimed to capture potential evidence for the upward propagation of acoustic-gravity waves into the ionosphere. A meteor radar and a very high frequency (VHF) coherent scattering radar operated by Wuhan University were located ~20 km southwest of the MVP-LAI system. These radars detected atmospheric temperature and density at ~80 km above the Earth's surface, and plasma irregularities at altitudes of approximately 90-160 km. The instrumental array also included a fluxgate magnetometer with a sampling rate of 10 Hz.

Variations in magnetic data, particularly in the horizontal component, are partially caused by changes in the electric current [Yamazaki et al., 2016] at an altitude of ~100 km above the MVP-LAI system. TEC variations in the ionosphere were monitored using ground-based GNSS receivers with sampling rates of 1 Hz or 50 Hz. Electromagnetic signals transmitted from geostationary satellites operated by the BeiDou navigation system (BDS) were primarily utilised to evaluate TEC (i.e., BDSTEC) in the ionosphere [Su et al., 2018; Chen et al., 2022b; Wang et al., 2023]. The BDS geostationary satellites are located ~36,000 km above the equator and can monitor changes in the TEC at particular ionospheric pierce points (IPPs) 24 h a day. The IPPs for the ground-based GNSS receiver in the MVP-LAI system were located ~250 km to the south. Other ground-based GNSS receivers were installed in the CAXI (31.8°N, 105.8°E) substation for the BDS G2 satellite, and in the YADU (31.9°N, 103.4°E) substation for the BDS G3 satellite. These GNSS receivers were used to monitor changes in TEC at IPPs immediately over the MVP-LAI system [Chen et al., 2022a].

To monitor potential chemical LAI coupling, the instrumental array included an emanometer, with a sampling interval of 10 mins, to monitor changes in radon concentration, and an atmospheric electric field meter with a sampling interval of 1 s to monitor the near-surface electric field. Precipitation measurements from an udometer and cloud observations from the Allsky camera were utilised to eliminate the influences of other factors in the lower atmosphere.

To consider LAI coupling via conductivity, variations in groundwater were recorded with a piezometer. Magnetic data from the magnetometer were also utilised to investigate the underlying conductivity of materials through the magnetic transfer transform [Parkinson and Jones, 1979; Chen, Hsu et al., 2013; Chen, Lin et al., 2015; Mao et al., 2020]. Air pressure and precipitation data from barometers and udometers were also considered to correct changes in groundwater levels because of the near-surface climate [Bredehoeft, 1967; Igarashi and Wakita, 1995; Kingsley et al., 2001; Van Der Kamp and Gale, 1983; Roeloffs, 1988; Chen, Wang et al., 2013; Orihara et al., 2014; Chen, Tang et al., 2015].

To explore potential electromagnetic LAI coupling, changes in the amplitude of the geomagnetic field in the frequency band of ~0.01 Hz were examined. Ground vibrations from seismometers were also compared with magnetic data to clarify potential causal mechanisms of the ground-electromagnetic coupling (i.e. motional induction, electrokinetic, and shaking effects) [Gao et al., 2016, 2020, 2021; Chen, Lin et al., 2021]. It is worth mentioning that the Hunga Tonga-Hunga Ha'apai (HTHH) volcano erupted on 15 January 2022, novel and/or hybrid channels dominate changes in the TEC have been identified and separated by the MVP-LAI system [Chen, Zhang et al., 2022; Sun et al., 2022; Chen et al., 2023]. The observation results show that the MVP-LAI system, with numerous instruments monitoring multiple parameters at distinct altitudes, has sufficient capability to capture signals related to LAI coupling.

3. Seismo-LAI coupling associated with the 2021 M7.4 Maduo earthquake

On 21 May 2021 the M6.4 Yangbi earthquake occurred in Yunnan, southwest China. Almost 4 h later, the M7.4 Maduo earthquake occurred in northwest China, approximately 1000 km away from the Yangbi earthquake. The Maduo earthquake was the largest earthquake in China after the 2008 M8.0 Wenchuan earthquake. Numerous studies have reported multiple abnormalities before the Maduo earthquake [Xie et al., 2021]. For example, Chen et al. [2022b] computed BDSTEC data at 850 motionless IPPs from 170 ground-based GNSS receivers, using electromagnetic signals transmitted from five BDS geostationary (G1-G5) satellites. They found temporary TEC perturbations associated with the Maduo earthquake over a wide area around the epicentre.

Here, we retrieved data from the same 170 ground-based GNSS receivers, operated by the Crustal Movement Observation Network of China. The GPS (Global Positioning System) TECs (i.e., GPSTECs) in this study were computed by comparing the pseudoranges and phases of the dual-frequency signals transmitted from the GPS orbiting satellites [Liu et al., 1996; Sun et al., 2013]. The GPSTEC average values computed utilizing a 1-hour moving window were removed from GPSTECs following the method in Chen et al. [2022b]; this processing mitigated interference mainly from solar activity.

Figure 2 shows the BDSTEC and GPSTEC perturbations associated with the Maduo earthquake from geostationary and orbiting satellites, respectively. Both BDSTEC and GPSTEC exhibit similar characteristics in regions far from earthquake epicentres (i.e., areas without earthquakes). In contrast, pronounced resident waves cannot be observed from GPSTEC data, but they are evident from the BDSTEC data. This suggests that signals from geostationary satellites are suitable for studying seismo-TEC anomalies. Chen et al. [2022b] explored potential mechanisms of LAI coupling via ground vibrations and TEC from the MVP-LAI system. Enhancements of the amplitudes at frequencies vary from low to high (~5×10^{-3} Hz), which can be consistently observed in the seismic and TEC data (Figures 3a and d). While the tendency of enhanced amplitudes to occur at high frequencies is consistent across major earthquakes worldwide [Chen, Lin et al., 2020, Chen et al., 2021c], the inference that TEC perturbations are triggered by ground vibrations lacks observational evidence linking changes on the ground to those in space.

We also collected air pressure and magnetic data from the MVP-LAI system during the same study period to investigate potential LAI coupling. These data were transformed into the frequency domain using a Fourier transform. Trends in the power spectral density function of the frequency were removed. The trend-free density was then smoothed, as shown in Figure 3. Figure 3 shows the time-frequency-power distributions of ground vibrations, air pressure, geomagnetic data, and TEC. Enhancements in the studied data (i.e. ground vibrations, air pressure, geomagnetic data, and TECs) occur at common frequencies of ~5×10^{-3} Hz a few days before earthquake occurrence. This frequency roughly agrees with the resonance frequency (~4×10^{-3} Hz) from the surface to the upper atmosphere [Chen, Saito et al., 2011; Dautermann et al., 2009; Liu et al., 2011; Matsumura et al., 2012; Saito et al., 2011]. This suggests that seismo-resonance LAI coupling is the driving mechanism behind the changes in ground vibrations, air pressure, geomagnetic data, and TEC.

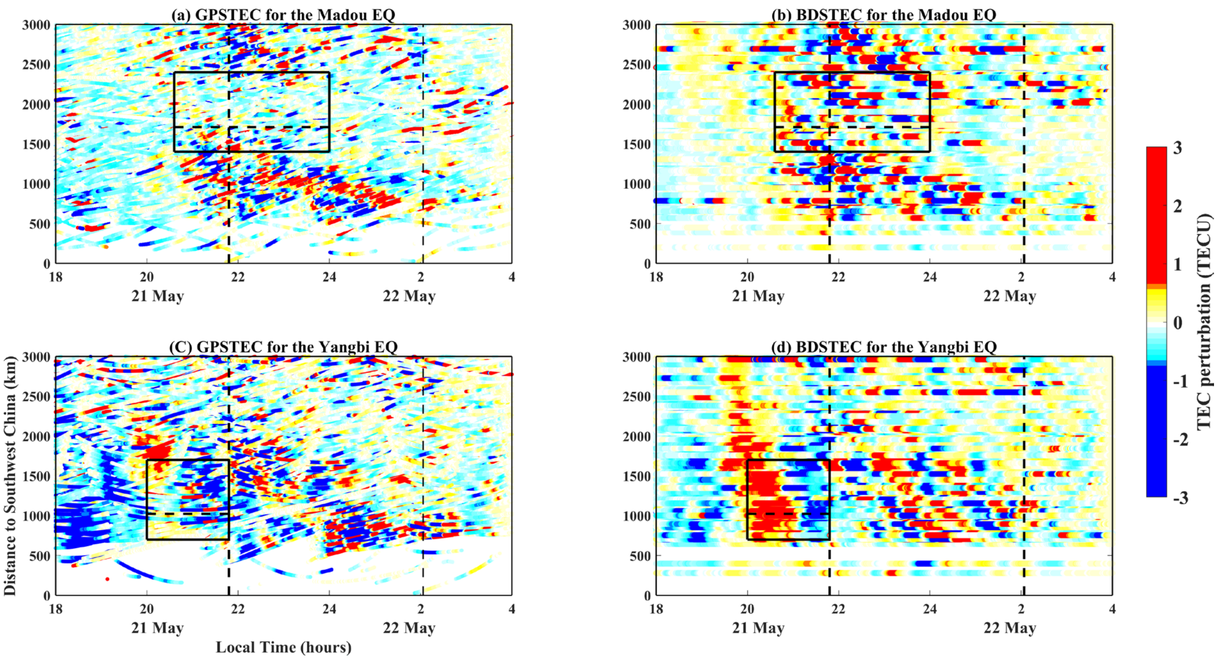

Figure 2. Spatiotemporal distribution of TEC perturbations during the Maduo and Yangbi earthquakes. TEC data are retrieved from 170 ground-based GNSS receivers in China (also see Chen et al., 2022b). TEC perturbations are computed by subtracting average (1-hour moving window) TEC values from each TEC datapoint. (a) and (c) show TEC perturbations obtained from the GPS orbiting satellites. (b) and (d) show TEC perturbations retrieved from the BDS geostationary satellites. The reference point for the distance axis is located in southwest China at (28°N, 90°E). The vertical dashed lines indicate occurrence of the Yangbi and Maduo earthquakes. The black rectangles show that the TEC pertubations cannot be obviously observed in data from the GPS orbiting satellites, but are observed in data from the BDS geostationary satellites.

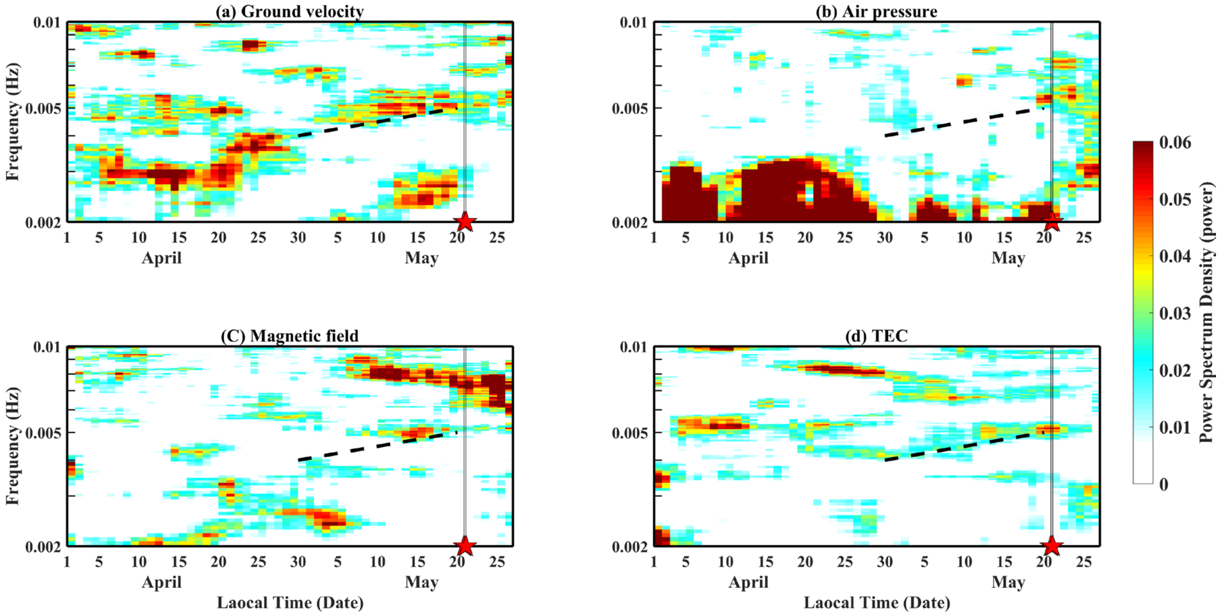

Figure 3. The time-frequency-spectrum distribution of the ground vibrations, air pressure, magnetic field, and TEC from the MVP-LAI system. The red stars and vertical lines indicate the Maduo and Yangbi earthquakes. The black dashed lines from Chen et al. [2022b], which indicate the spectra that tend to high frequencies before earthquake occurrence, are marked in Figures 3b and c for reference.

4. Double resonance before earthquakes

This study suggests that two resonance systems control the observed responses from multiple geophysical parameters. One resonance system exists in the lithosphere before the failure of the crust (i.e. fault dislocation). The other is atmospheric resonance, which affects multiple geophysical parameters (i.e. ground vibrations, air pressure, geomagnetic field, and TEC), all of which share frequencies close to $\sim 5 \times 10^{-3}$ Hz. Here, we discuss the potential relationship between the two resonance systems. Chen, Sun et al. [2020] reported that seismo-ground vibrations are distributed over a wide frequency band, mainly ranging between $\sim 10^{-4}$ Hz and $\sim 10^{-2}$ Hz. The frequencies of the vibrations are approximately consistent with the natural frequencies before material failure for a thin plate on the scale of a hundred kilometres [Leissa, 1969].

Lognonńe et al. [1998], Artu et al. [2004], and Dautermann et al. [2009] have reported that ground vibrations and air pressure are coupled (ground-air coupling) at a frequency of 3.4×10^{-3} Hz; this coupling comes from continuous seismic waves, particularly Rayleigh waves. The frequency range of 10^{-4} Hz-10^{-2} Hz reported by Chen, Sun et al. [2020] for ground vibrations before earthquakes include the frequency of 3.4×10^{-3} Hz that we identify for ground-air coupling. Therefore, we conclude that ground vibrations with variable frequencies occur on a hundred-kilometre scale several days before earthquakes [Bedford et al., 2020; Chen et al., 2011, Chen, Yeh et al., 2020]. Because of the similarity of the frequency of the ground vibrations and atmospheric resonance, these ground vibrations are a potential source of the atmospheric resonance before earthquakes. Therefore, double resonance is a key to the seismo-LAI coupling.

Infrasound can originate directly from large-scale ground vibrations. The vibrations trigger air-pressure changes owing to the air-ground coupling that generates atmospheric resonance and/or acoustic-gravity waves that propagate upward into the upper atmosphere. Liu et al. [2016a] reported that upward propagation of acoustic-gravity waves can drive changes in the magnetic field (due to the ionospheric current at $\sim$100 km altitude) and the TEC (in the ionosphere at $\sim$350 km altitude) as already suggested by Korepanov et al. [2009]. Therefore, persistent seismo-vibrations on a hundred-kilometre scale cause seismo-magnetic and-TEC anomalies over a wide area. The seismo-magnetic anomalies are caused by multiple sources simultaneously: (1) the direct contribution of ground vibrations due to the motional induction effect [Gao et al., 2014, 2019; Zhao et al., 2021; Chen Lin, et al., 2021] and the electrokinetic effect [Gao and Hu, 2010; Ren et al., 2015; Gao et al., 2016, 2020]; and (2) the changes in ionospheric currents at

~100 km altitude due to acoustic-gravity waves and atmospheric resonance [Korepanov et al., 2009; Liu et al., 2016a; Yamazaki et al., 2016; Chen et al., 2023].

Cloud shapes from an Allsky camera are another piece of evidence that partially supports acoustic-gravity waves and atmospheric resonance before earthquakes. Acoustic-gravity waves and atmospheric resonance affect clouds and induce railing shapes, also called earthquake clouds [Guo and Wang, 2008; Guo and Jie, 2013]. The enhancement of the near-surface electric field can be attributed to dust from atmospheric resonance [Dolezalek et al., 1974]. The relationship between earthquakes and the Schumann resonance in the upper atmosphere has been reported by numerous studies [Ohta et al., 2006, 2009; Ouyang et al., 2013; Hayakawa et al., 2021b]. The Schumann resonance may originate from high frequencies of atmospheric resonance. In short, multiple geophysical parameters (i.e. infrasound, near-surface electric field, cloud shape, electromagnetism, and TEC) can be attributed to persistent seismo-vibrations on a hundred-kilometre scale. The acoustic-gravity channel is therefore a promising candidate for seismo-LAI coupling. Thermal anomalies are not only sources for the acoustic-gravity variations observed but also for ground vibrations before earthquakes. Note that numerical simulations of acoustic-gravity waves generated by a point source on the ground have also been processed [Gao et al., 2023].

5. MVP-LAI in the near future

Observations associated with several earthquakes and the HTHH volcanic eruption have shown the capacity of the MVP-LAI system to monitor vibrations and perturbations in the LAI. However, the MVP-LAI system is insufficient [Hayakawa et al., 2023], and still limited in its observations of electromagnetic signals, infrasonic waves, and fluctuations in atmospheric layers at distinct altitudes. Observations of electromagnetic signals are limited to the frequency band between direct current (DC) and 10 Hz. Future inclusion of a magnetotelluric system will allow the MVP-LAI system to routinely monitor electromagnetic signals across a wide frequency band, as well as detect changes in the underlying electric current. These instruments would be helpful in studying seismo-electromagnetic anomalies in a relatively high frequency band, and exploring further the seismo-Schumann resonance in the upper atmosphere [Hayakawa et al., 2021b].

Infrasound will also be installed in the system to capture air pressure in a relatively low-frequency band, which is beneficial for the investigation of ground-air coupling. Ionosondes and high-frequency (HF) Doppler sounders will also be added to the MVP-LAI system to enhance the capacity for monitoring fluctuations in the atmospheric layers, which is important evidence for wave propagation. An additional substation for a ground-based GNSS receiver will also be established to receive electromagnetic signals transmitted from the BDS G1 satellite. Using different azimuths of GNSS receivers across three substations is beneficial for observing the TEC across the study area and studying wave propagation in different directions [Wang et al., 2023]. Indeed, using the MVP-LAI system at only one site (i.e. Leshan) was inefficient for monitoring the slant propagation of vibrations and perturbations. An additional one or two sites for the MVP-LAI system are required to form an MVP-LAI array. An array would not only facilitate confirmation of our observations, but also capture additional directions of vibrations and perturbations.

6. Conclusions

The MVP-LAI system, in conjunction with the BDS geostationary satellites, helped to alleviate the shortage of observation data between the ground and space in the past. The air pressure and magnetic data establish a link between ground vibrations in the lithosphere and TEC in the ionosphere, which allows us to investigate the potential mechanisms of the seismo-LAI coupling during earthquakes. The obtained evidence proposes a novel double-resonance mechanism to describe multiple geophysical parameters in seismo-LAI coupling: (1) ground vibrations occurring on the scale of a hundred kilometres, where crustal resonance happens due to material failure (i.e. fault dislocation); and (2) a common frequencies of $\sim 5 \times 10^{-3}$ Hz in air pressure, the magnetic field and TEC due to atmospheric resonance. The double resonance mechanism supports the anomalous geophysical parameters observed from the near-surface to the ionosphere, particularly for TEC and thermal anomalies distributing in wide areas reported in the previous studies. The development of a powerful method for sufficiently retrieving resonance signals from multiple parameters will play an important role in studying the double resonance in seismo-LAI coupling in the future.

Funding. This research was funded by the Joint Funds of the National Natural Science Foundation of China, grant number U2039205, Yunnan Provincial Science and technology department, key Program and development plan social development special (Public Security direction) science and technology project "Application research on key technologies of architecture safety risk prevention" grant number 202003AC100001, supported by Sichuan Scientific and technology, grant number 2020YFS0354, and the Special Training Project of National Science Foundation of Xinjiang Uygur Autonomous Region, grant number 2022D03031.

Availability Statements. TEC and magnetic data were retrieved from China Earthquake Networks Center and National Earthquake Data Center; China. Magnetic data with tilt data are retrieved from Institute of Earth Sciences, Academia Sinica, Taiwan. Data from the MVP-LAI system are obtained from Institute of Geophysics and Geomatics, China University of Geosciences, Wuhan.

Acknowledgements. The authors thank that China Earthquake Networks Center; National Earthquake Data Center; and Academia Sinica in China provided data. We thank the people who established and maintain the MVP-LAI system and provided data.

References

Artru, J., T. Farges and P. Lognonn'e (2004). Acoustic Waves generated from seismic surface waves: Propagation properties determined from Doppler sounding observations and normal-mode modeling, Geophys. J. Int., 158, 1067-1077.

Astafyeva, E., S. Shalimov, E. Olshanskaya and P. Lognonne (2013). Ionospheric response to earthquakes of different magnitudes: Larger quakes perturb the ionosphere stronger and longer, Geophys. Res. Lett., 40, 1675-1681, 2013.

Astafyeva, E. (2019). Ionospheric detection of natural hazards, Rev. Geophys., 57, 1265-1288, https://doi.org/10.1029/2019RG000668.

Bedford, J.R., M. Moreno, Z. Deng, O. Oncken, B. Schurr, T. John, J.C. Báez and M. Bevis (2020). Months-long thousand-kilometre-scale wobbling before great subduction earthquakes, Nature, 580, 628-635.

Bishop, R.L. and P.R. Straus (2006). Characterizing ionospheric variations in the vicinity of hurricanes and typhoons using GPS occultation measurements, AGU Fall Meeting, San Francisco, 11-15 December, Eos (Trans Am Geophys Union), 87(Suppl.):SA33B-0276.

Blackett, M., M.J. Wooster and B.D. Malamud (2011) Exploring land surface temperature earthquake precursors: A focus on the Gujarat (India) earthquake of 2001, Geophys. Res. Lett., 38, 303.

Bleier, T.E., C. Dunson, M. Maniscalco, N. Bryant, R. Bambery and F. Freund (2009). Investigation of ULF magnetic pulsations, air conductivity changes, and infrared signatures associated with the 30 October Alum Rock M5.4 earthquake, Nat. Hazards Earth Syst. Sci., 9, 585-603.

Bredehoeft, J.D. (1967). Response of well-aquifer systems to Earth tides, J. Geophys. Res., 72, 3075-3087.

Chakrabarti, S.K. (2010). Propagation Effects of Very Low Frequency Radio Waves, Conference Proceedings 1286, American Institute of Physics.

Chen, C.H., H.L. Hsu, S. Wen, T.K. Yeh, F.Y. Chang, C.H. Wang, J.Y. Liu, Y.Y. Sun, K. Hattori, H.Y. Yen and P. Han (2013). Evaluation of seismo-electric anomalies using magnetic data in Taiwan, Nat. Hazards Earth Syst. Sci., 13, 597-604, https://doi.org/10.5194/nhess-13-597-2013.

Chen, C.H., C.H. Lin, C.H. Wang, J.Y. Liu, T.K. Yeh, H.Y. Yen and T.W. Lin (2015). Potential relationships between seismo-deformation and seismo-conductivity anomalies, J. Asian Earth Sci., 114, 327-337, https://doi.org/10.1016/j.jseaes.2015.03.023.

Chen, C.-H., J.-Y. Lin, Y. Gao, C.-H. Lin, P. Han, C.-R. Chen, L.-C. Lin, R. Huang and J.-Y. Liu (2021). Magnetic pulsations triggered by microseismic ground motion, J. Geophys. Res. 126, e2020JB021416, https://doi.org/10.1029/2020JB021416.

Chen, C.-H., L.-C. Lin, T.K. Yeh, S. Wen, H. Yu, Y. Chen, Y. Gao, P. Han, Y.-Y. Sun, J.-Y. Liu, C.-H. Lin, C.-C. Tang, C.-M. Lin, H.-H. Hsieh and P.-J. Lu (2020). Determination of epicenters before earthquakes utilizing far seismic and GNSS data: Insights from ground vibrations, Remote Sens., 12, 3252, https://doi.org/10.3390/rs12193252.

Chen, C.H., A. Saito, C.H. Lin, J.Y. Liu, H.F. Tsai, T. Tsugawa, et al. (2011). Long-distance propagation of ionospheric disturbance generated by the 2011 off the Pacific coast of Tohoku earthquake, Earth Planets and Space, 63(7), 881-884, https://doi.org/10.5047/eps.2011.06.026.

Chen, C.-H., Y.-Y. Sun, K. Lin, J. Liu, Y. Wang, Y. Gao, D. Zhang, R. Xu and C. Chen (2021c). The LAI Coupling Associated with the M6 Luxian Earthquake in China on 16 September 2021, Atmosphere, 12(12), 1621, https://doi.org/10.3390/atmos12121621.

Chen, C.-H., Y.-Y. Sun, K. Lin, C. Zhou, R. Xu, H. Qing, Y. Gao, T. Chen, F. Wang, H. Yu, P. Han, C.-C. Tang, X. Su, X. Zhang, L. Yuan, Y. Xu and J.-Y. Liu (2021b). A new instrumental array in Sichuan, China, to monitor vibrations and perturbations of the lithosphere, atmosphere and ionosphere, Surv. Geophys., 42, 1425-1442, https://doi.org/10.1007/s10712-021-09665-1.

Chen, C.-H., Y.-Y. Sun, L.-C. Lin, P. Han, H. Yu, X. Zhang, C.-C. Tang, C.-R. Chen, H.Y. Yen, C.-H. Lin, J.Y. Liu and C.-R. Lin (2021a). Large air pressure changes triggered by P-SV ground motion in a cave in northern Taiwan, Sci. Rep., 11, 12850, https://doi.org/10.1038/s41598-021-92216-w.

Chen, C.-H., Y.-Y. Sun, S. Wen, P. Han, L.-C. Lin, H. Yu, X. Zhang, Y. Gao, C.-C. Tang, C.-H. Lin and J.-Y. Liu (2020). Spatiotemporal changes of seismicity rate during earthquakes, Nat. Hazards Earth Syst. Sci., 20, 3333-3341, https://doi.org/10.5194/nhess-20-3333-2020.

Chen, C.-H., Y.-Y. Sun, X. Zhang, Y. Gao, F. Wang, K. Lin, C.-C. Tang, R. Huang, R. Xu, J. Liu, Y. Wang and C. Chen (2022a). Resonant signals in the lithosphere-atmosphere-ionosphere coupling, Sci. Rep., 12, 14587, https://doi.org/10.1038/s41598-022-18887-1.

Chen, C.-H., Y.-Y. Sun, R. Xu, K. Lin, F. Wang, D. Zhang, Y. Zhou, Y. Gao, X. Zhang, H. Yu and J.-Y. Liu (2022b). Resident waves in the ionosphere before the M6.1 Dali and M7.3 Qinghai earthquakes of 21-22 May 2021, Earth Space Sci., 9, e2021EA002159, https://doi.org/10.1029/2021EA002159.

Chen, C.-H., Y.-Y. Sun, X. Zhang, F. Wang, K. Lin, Y. Gao, C.-C. Tang, J. Lyu, R. Huang and Q. Huang (2023). Far-field coupling and interactions in multiple geospheres after the Tonga volcano eruptions, Surv. Geophys., 44, 587-601, https://doi.org/10.1007/s10712-022-09753-w.

Chen, C.H., C.C. Tang, K.C. Cheng C.H. Wang, S. Wen, C.H. Lin, Y.Y. Wen, G. Meng, T.K. Yeh, J.C. Jan, H.Y. Yen and J.Y. Liu (2015). Groundwater-strain coupling before the 1999 Mw 7.6 Taiwan Chi-Chi earthquake, J. Hydrol., 524, 378-384, https://doi.org/10.1016/j.jhydrol.2015.03.006.

Chen, C.H., C.H. Wang, S. Wen, T.K. Yeh, C.H. Lin, J.Y. Liu, H.Y. Yen, C. Lin, R.J. Rau and T.W. Lin (2013). Anomalous frequency characteristics of groundwater level before major earthquake in Taiwan, Hydrol. Earth Syst. Sc., 17, 1693-1703, https://doi.org/10.5194/hess-17-1693-2013.

Chen, C.H., T.K. Yeh, J.Y. Liu, C.H. Wang, S. Wen, H.Y. Yen and S.H. Chang (2011). Surface Deformation and Seismic Rebound: implications and applications, Surv. Geophys., 32(3), 291-313, https://doi.org/10.1007/s10712-011-9117-3.

Chen, C.-H., T.-K. Yeh, S. Wen, G. Meng, P. Han, C.-C. Tang, J.-Y. Liu and C.-H. Wang (2020). Unique Pre-Earthquake Deformation Patterns in the Spatial Domains from GPS in Taiwan, Remote Sens., 12, 366, https://doi.org/10.3390/rs12030366.

Chen, C.-H., X. Zhang, Y.-Y. Sun, F. Wang, T.-C. Liu, C.-Y. Lin, Y. Gao, J. Lyu, X. Jin, X. Zhao, X. Cheng, P. Zhang, Q. Chen, D. Zhang, Z. Mao and J.-Y. Liu (2022). Individual wave propagations in ionosphere and troposphere triggered by the Hunga Tonga-Hunga Ha'apai underwater volcano eruption on 15 January 2022, Remote Sens., 14, 2179, https://doi.org/10.3390/rs14092179.

Chen, H., R. Wang, M. Miao, X. Liu, Y. Ma, K. Hattori and P. Han (2020). A Statistical Study of the Correlation between Geomagnetic Storms and M ≥ 7.0 Global Earthquakes during 1957-2020, Entropy, 22(11), 1270.

Chen, T., L. Li, X.-X. Zhang, Q.-M. Ma, W. Li, S. Ti, H. Wu, R.-K. Li, J. Luo and J.-F. Su (2022). Near-epicenter weather conditions several hours before strong earthquakes (Ms 6), Nat. Hazards, 110, 57-68.

Chen, Y.-I., C.-S. Huang and J.Y. Liu (2015). Statistical evidences of seismo-ionospheric precursors applying receiver operating characteristic (ROC) curve on the GPS total electron content in China, J. Asian Earth Sci., 114, 393-402.

Cho, M. and M.J. Rycroft (1998). Computer simulation of the electric field structure and optical emission from cloud-top to the ionospheres, J. Atmos. Sol.-Terr. Phys., 60, 871-888, 1998.

Chou, M.Y., C.C.H. Lin, J. Yue, L.C. Chang, H.F. Tsai and C.H. Chen (2017b). Medium-scale traveling ionospheric disturbances triggered by Super Typhoon Nepartak (2016). Geophys. Res. Lett., 44, 7569-7577, https://doi.org/10.1002/2017GL073961

Chou, M.Y., C.C.H. Lin, J. Yue, H.F. Tsai, Y.Y. Sun, J.Y. Liu and C.H. Chen (2017a). Concentric traveling ionosphere disturbances triggered by Super Typhoon Meranti (2016). Geophys. Res. Lett., 44, 1219-1226, https://doi.org/10.1002/2016GL072205

Chou, M.Y., I. Cherniak, C.C.H. Lin and N.M. Pedatella (2020). The persistent ionospheric responses over Japan after the impact of the 2011 Tohoku earthquake, Space Weather, 18, e2019SW002302, https://doi.org/10.1029/2019SW002302.

Choudhury, S., S. Dasgupta, A.K. Saraf and S.K. Panda (2006). Remote sensing observations of pre-earthquake thermal anomalies in Iran, Int. J. Remote Sens., 27, 4381-4396.

Chum, J., Y.J. Liu, J. Laštovička, J. Fišer, Z. Mošna, J. Baše and Y.Y. Sun (2016). Ionospheric signatures of the April 25, 2015 Nepal earthquake and the relative role of compression and advection for Doppler sounding of infrasound in the ionosphere, Earth Planets Space, 68, 24, https://doi.org/10.1186/s40623-016-0401-9.

Dautermann, T., E. Calais, P. Lognonné and G.S. Mattioli (2009). Lithosphere—Atmosphere—ionosphere coupling after the 2003 explosive eruption of the Soufriere Hills Volcano, Montserrat, Geophys. J. Int., 179, 1537-1546, https://doi.org/10.1111/j.1365-246X.2009.04390.x.

Davies, K. (1990). Ionospheric Radio, Peregrinus, London.

De la Torre, A., P. Alexander and A. Giraldez (1999). The kinetic to potential energy ratio and spectral separability from high-resolution balloon soundings near the Andes Mountains, Geophys. Res. Lett., 26, 1413-1416.

Dolezalek, H., R. Reiter and H.E. Landsberg (1974). Electrical processes in atmospheres, Steinkopff, Heidelberg.

Dunajecka, M.A. and S.A. Pulinets (2005). Atmospheric and thermal anomalies observed around the time of strong earthquakes in México, Atmósfera, 18(4), 235-247.

Ellsworth, W.L. and G.C. Beroza (1995). Seismic evidence for an earthquake nucleation phase, Science, 268, 851-855.

Fraser-Smith, A.C., A. Bernardi, P.R. McGill, M.E. Ladd, R.A. Helliwell, and O.G. Villard (1990). Low-frequency magnetic field measurements near the epicenter of the M_S7.1 Loma Prieta earthquake, Geophys. Res. Lett., 17(9), 1465-1468, https://doi.org/10.1029/GL017i009p01465.

Freund, F.T., M.R. Mansouri Daneshvar and M. Ebrahimi (2022) Atmospheric Storm Anomalies Prior to Major Earthquakes in the Japan Region, Sustainability, 14, 10241, https://doi.org/10.3390/su141610241.

Gao, Y. and H. Hu (2010). Seismoelectromagnetic waves radiated by a double couple source in a porous medium, Geophys. J. Int., 181, 873-896.

Gao, Y., X. Chen, H. Hu, J. Wen, J. Tang and G. Fang (2014). Induced electromagnetic field by seismic wave in earth's magnetic field, J. Geophys. Res. Solid Earth, 119, 5651-5685, https://doi.org/10.1002/2014JB010962.

Gao, Y., J.M. Harris, J. Wen, Y. Huang, C. Twardzik, X. Chen and H. Hu (2016). Modeling of the coseismic electromagnetic fields observed during the 2004 Mw 6.0 Parkfield earthquake, Geophys. Res. Lett., 43, 620-627. https://doi.org/10.1002/2015GL067183.

Gao, Y., P. Jiang, Y. Xu, L. Jiang, C.H. Chen, G. Zhao, J. Tang, X. Chen B. Han, J. Chong and C. Yao (2021). On magnetic disturbances induced by rotation of coil-type magnetometer driven by seismic waves, Geophys. J. Int., 226, 1948-1974, https://doi.org/10.1093/gji/ggab190.

Gao, Y., T. Li, G. Zhou, C.-H. Chen, Y.-Y. Sun, X. Zhang, J.-Y. Liu, J. Wen, C. Yao and X. Bai (2023). Acoustic-gravity waves generated by a point source on the ground in a stratified atmosphere-Earth structure, Geophys. J. Int., 232, 764-787, https://doi.org/10.1093/gji/ggac364.

Gao, Y., D. Wang, J. Wen, H. Hu, X. Chen and C. Yao (2019). Electromagnetic responses to an earthquake source due to the motional induction effect in a 2D layered model, Geophys. J. Int., 219(1), 563-593. https://doi.org/10.1093/gji/ggz303.

Gao, Y., G. Zhao, J. Chong, S.L. Klemperer, B. Han, F. Jiang, J. Wen, X. Chen, Y. Zhan, J. Tang, Q. Xiao and L. Wang (2020). Coseismic electric and magnetic signals observed during 2017 Jiuzhaigou Mw 6.5 earthquake and explained by electrokinetics and magnetometer rotation, Geophys. J. Int., 223(2), 1130-1143.

Genzano, N., C. Filizzola, K. Hattori, N. Pergola and V. Tramutoli (2021). Statistical correlation analysis between thermal infrared anomalies observed from MTSATs and large earthquakes occurred in Japan (2005-2015), J. Geophys. Res. Solid Earth, 126, e2020JB020108.

Gokhberg, M.B., I.L. Gufeld, A.A. Rozhnoi, V.F. Marenko, V.S. Yampolsky and E.A. Ponomarev (1989). Study of seismic influence on the ionosphere by super long wave probing of the Earth-ionosphere waveguide, Phys. Earth Planet. Inter., 57, 64-67.

Gufeld, I.L., A.A. Rozhnoi, S.N. Tyumensev, S.V. Sherstuk and V.S. Yampolsky (1992). Radiowave disturbances in period to Rudber and Rachinsk earthquakes, Phys. Solid Earth, 28(3), 267-270.

Guo, G.M. and Y. Jie (2013). Three attempts of earthquake prediction with satellite cloud images, Nat. Hazards Earth Syst. Sci., 13, 91-95.

Guo, G.M. and B. Wang (2008). Cloud anomaly before Iran earthquake, Int. J. Remote Sens., 2, 1921-1928.

Hadjicontis, V., C. Mavromatou and D. Ninos (2004). Stress induced polarization currents and electromagnetic emission from rocks and ionic crystals, accompanying their deformation, Nat. Hazards Earth Syst. Sci., 4 (5/6), 633-639.

Han, P., K. Hattori, M. Hirokawa, J. Zhuang, C.H. Chen, F. Febriani, H. Yamaguchi, C. Yoshino, J.Y. Liu and S. Yoshida (2014). Statistical analysis of ULF seismo-magnetic phenomena at Kakioka, Japan, during 2001-2010, J. Geophys. Res. Space Physics, 119, 4998-5011, https://doi.org/10.1002/2014JA019789.

Han, P., K. Hattori, J. Zhuang, C.H. Chen, J.Y. Liu and S. Yoshida (2017). Evaluation of ULF seismo-magnetic phenomena in Kakioka, Japan by using Molchan's error diagram, Geophys. J. Int., 208, 482-490, https://doi.org/10.1093/gji/ggw404.

Harrison, R.G., K.L. Aplin and M.J. Rycroft (2010). Atmospheric electricity coupling between earthquake regions and the ionosphere, J. Atmos. Sol.-Terr. Phys., 72, 376-381.

Harrison, R.G., K.L. Aplin and M.J. Rycroft (2014). Brief Communication: Earthquake-cloud coupling through the global atmospheric electric circuit, Nat. Hazards Earth Syst. Sci., 14, 773-777, https://doi.org/10.5194/nhess-14-773-2014.

Hattori, K. and P. Han (2018). Statistical Analysis and Assessment of Ultralow Frequency Magnetic Signals in Japan As Potential Earthquake Precursors, in Pre-Earthquake Processes: A Multidisciplinary Approach to Earthquake Prediction Studies D. Ouzounov, S. Pulinets, K. Hattori and P. Taylor (Editors), American Geophysical Union by John Wiley & Sons, Inc..

Hattori, K., P. Han, C. Yoshino, F. Febriani, H. Yamaguchi and C.H. Chen (2013). Investigation of ULF Seismo-Magnetic Phenomena in Kanto, Japan During 2000-2010: Case Studies and Statistical Studies, Surv. Geophys., 34, 293-316, https://doi.org/10.1007/s10712-012-9215-x.

Hayakawa, M. and Y. Hobara (2010). Current status of seismo-electromagnetics for short-term earthquake prediction, Geomatics Nat. Hazards Risk., 1(2), 115-155.

Hayakawa, M., J. Izutsu, A. Yu Schekotov, A.P. Nickolaenko, YuP. Galuk and I.G. Kudintseva (2021b) Anomalies of Schumann resonances as observed near Nagoya associated with two huge (M~7) Tohoku offshore earthquakes in 2021, J. Atmos. Sol.-Terr. Phys., 225, 105761.

Hayakawa, M., J. Izutsu, A. Schekotov, S.-S. Yang, M. Solovieva and E. Budilova (2021a). Lithosphere-Atmosphere-Ionosphere Coupling Effects Based on Multiparameter Precursor Observations for February-March 2021 Earthquakes (M~7) in the Offshore of Tohoku Area of Japan, Geosciences, 11, 481, https://doi.org/10.3390/geosciences11110481.

Hayakawa, M., O.A. Molchanov, T. Ondoh and E. Kawai (1996). The precursory signature effect of the Kobe earthquake on VLF subionospheric signals, J. Comm. Res. Lab Tokyo, 43:169-180.

Hayakawa, M., T. Nakamura, Y. Hobara and E. Williams (2004). Observation of sprites over the Sea of Japan and conditions for lightning-induced sprites in winter, J. Geophys. Res. Space Phys, 109, A01312. https://doi.org/10.1029/2003JA009905.

Hayakawa, M., A. Schekotov, J. Izutsu, S.-S. Yang, M. Solovieva and Y. Hobara (2022). Multi-Parameter Observations of Seismogenic Phenomena Related to the Tokyo Earthquake (M = 5.9) on 7 October 2021, Geosciences, 12, 265, https://doi.org/10.3390/geosciences12070265.

Hayakawa, M., A. Schekotov, J. Izutsu, A.P. Nickolaenko and Y. Hobara (2023). Seismogenic ULF/ELF Wave Phenomena: Recent Advances and Future Perspectives. Open J. Earthq. Res., 12, 45-113, https://doi.org/10.4236/ojer.2023.123003.

Hayakawa, M. (2016). Earthquake prediction with electromagnetic phenomena, Aip Conference Proceedings.

Hayakawa, M. (2015). Earthquake Prediction with Radio Techniques, JohnWiley & Sons, Singapore Pte Ltd, Singapore.

Hayakawa, M. (2011). Probing the lower ionospheric perturbations associated with earthquakes by means of subionospheric VLF/LF propagation, Earthquake Sci., 24(6), 609-637.

Hayakawa, M. (2007). VLF/LF radio sounding of ionospheric perturbations associated with earthquakes, Sensors, 7, 1141-1158.

Hickey, M.P., G. Schubert and R.L. Walterscheid (2001). Acoustic wave heating of the thermosphere, J. Geophys. Res. Space Phys., 106(A10), 21543-21548, https://doi.org/doi:10.1029/2001ja000036.

Huang, Y.N., K. Cheng and S.W. Chen (1985). On the detection of acoustic-gravity waves generated by typhoon by use of real time HF Doppler frequency shift sounding system, Radio Sci., 20, 897-906, https://doi.org/10.1029/RS020i004p00897.

Igarashi, G. and H. Wakita (1995). Geochemical and hydrological observations for earthquake prediction in Japan, J. Phys. Earth, 43, 585-598.

Inan, U.S., T.F. Bell and J.V. Rodriguez (1991). Heating and ionization of the lower ionosphere by lightning, Geophys. Res. Lett., 18, 705-708.

Hao, J. (1989). Near earth surface anomalies of the atmospheric electric field and earthquakes, Acta Seismol. Sin. Engl. Ed., 2, 289-298.

Kai, Q. (2012). Preliminary analysis of surface temperature anomalies that preceded the two major Emilia 2012 earthquakes (Italy), Ann. Geophys, 55, 823-828.

Kasahara, K. (1981). Earthquake mechanics. Cambridge University Press, Cambridge.

Kasahara, Y., T. Nakamura, Y. Hobara, M. Hayakawa, A. Rozhnoi, M. Solovieva and O.A. Molchanov (2010). A statistical study on the AGW modulation in subionospheric VLF/LF propagation data and consideration of the generation mechanism of seismo-ionospheric perturbations, J. Atmos. Electr., 30(2), 103-112.

Kelley, M.C., W.E. Swartz and K. Heki (2017). Apparent ionospheric total electron content variations prior to major earthquakes due to electric fields created by tectonic stresses, J. Geophys. Res. Space Phys., 122, 6689-6695, https://doi.org/10.1002/2016JA023601.

Kingsley, S.P., P.E. Biagi, R. Piccolo, V. Capozzi, A. Ermini, Y.M. Khatkevich, and E.I. Gordeev (2001). Hydrogeochemical precursors of strong earthquakes: a realistic possibility in Kamchatka, Phy. Chem. Earth, 26, 769-774.

Korepanov, V., M. Hayakawa, Y. Yampolski and G. Lizunov (2009). AGW as a seismo-ionospheric coupling responsible agent, Phys. Chem. Earth, 34(6-7), 485-495.

Laštovička, J. and T. Šindelářová (2019). Large-Scale and Transient Disturbances and Trends: From the Ground to the Ionosphere, in Infrasound Monitoring for Atmospheric Studies A. Le Pichon, E. Blanc and A. Hauchecorne (Editors), Springer, Cham, https://doi.org/10.1007/978-3-319-75140-5_25.

Leissa, A.W. (1969). Vibrations of Plates; Ohio State University, Columbus, OH, USA.

Liu, J., X. Qiao, X. Zhang, Z. Wang, C. Zhou and Y. Zhang (2022). Using a Spatial Analysis Method to Study the Seismo-Ionospheric Disturbances of Electron Density Observed by China Seismo-Electromagnetic Satellite, Front. Earth Sci., 10, 811658, https://doi.org/10.3389/feart.2022.811658.

Liu, J.Y., C.H. Chen, Y.Y. Sun, C.H. Chen, H.F. Tsai, H.Y. Yen, J. Chum, J. Lastovicka, Q.S. Yang, W.S. Chen and S. Wen (2016a). The vertical propagation of disturbances triggered by seismic waves of the 11 March 2011 M9.0 Tohoku Earthquake over Taiwan, Geophys. Res. Lett., 43, 1759-1765, https://doi.org/10.1002/2015GL067487.

Liu, J.Y., Y.I. Chen, C.H. Huang, Y.Y. Ho and C.H. Chen (2016). A statistical study of lightning activities and M ≧ 5.0 earthquakes in Taiwan during 1993-2004, Surv. Geophys., 36, 851-859, https://doi.org/10.1007/s10712-015-9342-2.

Liu, J.Y., Y. Tsai, C. Chen, Y. Chen and H. Yen (2016b). Integrated search for Taiwan earthquake precursors (ISTEP), IEEJ Trans. Fund. Mater., 136(5), 214-220, https://doi.org/doi:10.1541/ieejfms.136.214.

Liu, J.Y., K. Wang, C.H. Chen, W.H. Yang, Y.H. Yen, Y.I. Chen, K. Hattori, H.T. Su, R.R. Hsu and C.H. Chang (2013). A statistical study on ELF-whistlers/emissions and M ≧ 5.0 earthquakes in Taiwan, J. Geophys. Res. 118, 3760-3768, https://doi.org/10.1002/jgra.50356.

Liu, J.-Y., C.-H. Chen, C.-H. Lin, H.-F. Tsai, C.-H. Chen and M. Kamogawa (2011). Ionospheric disturbances triggered by the 11 March 2011M9.0 Tohoku earthquake, J. Geophys. Res., 116, A06319, https://doi.org/10.1029/2011JA016761.

Liu, J.Y., Y.B. Tsai, S.W. Chen, C.P. Lee, Y.C. Chen, H.Y. Yen, W.Y. Chang and C. Liu (2006). Giant ionospheric disturbances excited by the M9.3 Sumatra earthquake of 26 December 2004, Geophys. Res. Lett., 33, L02103. https://doi.org/10.1029/2005GL023963.

Liu, J.Y., H.F. Tsai and T.K. Jung (1996). Total electron content obtained by using the Global Positioning System, Terr. Atmos. Ocean Sci., 7, 107-117.

Lognonńe, P., E. Cĺevede and H. Kanamori (1998). Computation of seismograms and atmospheric oscillations by normal-mode summation for a spherical earth model with realistic atmosphere, Geophys. J. Int., 135, 388-406.

Ma, J. (2016). Whether earthquake precursors help for prediction do exist, Sci. China Press Chin. Ed., 61, 409-414.

Mao, Z.Q., C.-H. Chen, S.Q. Zhang, A. Yisimayili, H.Z. Yu, C. Yu and J.-Y. Liu (2020). Locating Seismo-Conductivity Anomaly before the 2017 M_W 6.5 Jiuzhaigou Earthquake in China Using Far Magnetic Stations, Remote Sens., 12, 1777, https://doi.org/10.3390/rs12111777.

Matsumura, M., H. Shinagawa and T. Iyemori (2012). Horizontal extension of acoustic resonance between the ground and the lower thermosphere, J. Atmos. Sol.-Terr. Phys., 75-76, 127-132.

Miyaki, K., M. Hayakawa and O.A. Molchanov (2002). The role of gravity waves in the lithosphere-ionosphere coupling, as revealed from the subionospheric LF propagation data, in Seismo-Electromagnetics (Lithosphere-Atmosphere-Ionosphere Coupling) M. Hayakawa and O.A. Molchanov (Ediotrs), Terra Scientific Publishing, Tokyo, 229-232.

Molchanov, O.A. and M. Hayakawa (1995). Generation of ULF electromagnetic emissions by microfracturing, Geophys. Res. Lett., 22, 3091-3094.

Molchanov, O.A. and M. Hayakawa (1998). Subionospheric VLF signal perturbations possibly related to earthquakes, J. Geophys. Res., 103, 17489-17504.

Molchanov, O.A., M. Hayakawa and K. Miyaki (2001). VLF/LF sounding of the lower ionosphere to study the role of atmospheric oscillations in the lithosphere-ionosphere coupling, Adv. Polar Upper Atmos. Res. Tokyo, 15, 146-158.

Molchanov, O.A., M. Hayakawa and V.A. Rafalsky (1995). Penetration characteristics of electromagnetic emissions from an underground seismic source into the atmosphere, ionosphere and magnetosphere, J. Geophys. Res., 100, 1691-1712.

Molchanov, O.A., O.A. Mazhaeva, A.N. Goliavin and M. Hayakawa (1993). Observations by the intercosmos-24 satellite of ELF-VLF electromagnetic emissions associated with earthquakes, Ann. Geophys., 11, 431-440.

Nishioka, M., T. Tsugawa and M. Kubota, et al. (2013). Concentric waves and short-period oscillations observed in the ionosphere after the 2013 Moore EF5 tornado, Geophys. Res. Lett., 40(21), 5581-5586, https://doi.org/10.1002/2013GL057963.

Ohta, K., J. Izutsu and M. Hayakawa (2009). Anomalous excitation of Schumann resonances and additional anomalous resonances before the 2004 Mid-Niigata prefecture earthquake and the 2007 Noto Hantou Earthquake, Phys. Chem. Earth, 34, 441-448.

Ohta, K., N. Watanabe and M. Hayakawa (2006). Survey of anomalous Schumann resonance phenomena observed in Japan, in possible association with earthquakes in Taiwan, Phys. Chem. Earth, 31, 397-402.

Orihara, Y., M. Kamogawa and T. Nagao (2014). Preseismic Changes of the level and temperature of confined groundwater related to the 2011 Tohoku earthquake, Sci. Rep., 4, 6907.

Ouyang, X., X. Zhang, A.P. Nickolaenko, M. Hayakawa, X. Shen and Y. Mao (2013). Schumann resonance observation in China and anomalous disturbance possibly associated with Tohoku M9.0 earthquake, Earthquake Science, 26(2), 137-145.

Ouzounov, D., N. Bryant, T. Logan, S. Pulinets and P. Taylor (2006). Satellite thermal IR phenomena associated with some of the major earthquakes in 1999-2004, Phys. Chem. Earth, 31, 154-163.

Ouzounov, D., D. Liu, C. Kang, G. Cervone, M. Kafatos and P. Taylor (2007). Outgoing long wave radiation variability from IR satellite data prior to major earthquakes, Tectonophysics, 431, 211-220.

Ouzounov, D., S. Pulinets, K. Hattori and P. Taylor (2018). Pre-Earthquake Processes: A Multidisciplinary Approach to Earthquake Prediction Studies, American Geophysical Union by John Wiley & Sons, Inc..

Oyama, K.I., Y. Kakinami, J.Y. Liu, M. Kamogawa and T. Kodama (2008). Reduction of electron temperature in low-latitude ionosphere at 600 km before and after large earthquakes, J. Geophys. Res., 113, A11317, http://doi.org/10.1029/2008JA013367.

Parkinson, W.D. and F.W. Jones (1979). The geomagnetic coast effect, Rev. Geophys., 17, 1999-2015.

Pasko, V.P., U.S. Inan, T.F. Bell and Y.N. Taranenko (1997). Sprites produced by quasi-electrostatic heating and ionization in the lower ionosphere, J. Geophys. Res. Space Phys., 102(A3), 4529-4561, http://doi.org/10.1029/96JA03528.

Polyakova, A.S. and N.P. Perevalova (2011). Investigation into impact of tropical cyclones on the ionosphere using GPS sounding and NCEP/NCAR Reanalysis data, Adv. Space Res., 48, 1196-1210.

Pulinets, S.A., A.V. Karelin, K.A. Boyarchuk and L.A. Pokhmelnykh (2006). The physical nature of thermal anomalies observed before strong earthquakes, Phys. Chem. Earth, 31, 143-153.

Pulinets, S.A. and K. Boyarchuk (2004). Ionospheric Precursors of Earthquakes, Springer, Berlin.

Pulinets, S.A. and D. Ouzounov (2011). Lithosphere-atmosphere-ionosphere coupling (LAIC) model—a unified concept for earthquake precursors validation, J. Asian Earth Sci., 41, 371-382.

Qin, K., L. Wu, A. De Santis and H. Wang (2011) Surface latent heat flux anomalies before the MS 7.1 New Zealand earthquake 2010, Chin. Sci. Bull., 56, 3273.

Rajesh, P.K., C.H. Lin, C.Y. Lin, C.H. Chen, J.Y. Liu, T. Matsuo, S.P. Chen, W.H. Yeh and C.Y. Huang (2021). Extreme positive ionosphere storm triggered by a minor magnetic storm in deep solar minimum revealed by formosat-7/cosmic-2 and GNSS observations, J. Geophys. Res. Space Phys., 126, e2020JA028261, http://doi.org/10.1029/2020JA028261.

Reasenberg, P.A. (1999). Foreshock occurrence before large earthquakes, J. Geophys. Res., 104, 4755-4768.

Ren, H., J. Wen, Q. Huang and X. Chen (2015). Electrokinetic effect combined with surface-charge assumption: A possible generation mechanism of coseismic EM signals, Geophys. J. Int., 200, 837-850.

Rishbeth, H. (2006). F-region links with the lower atmosphere? J. Atmos. Sol.-Terr. Phys., 68, 469-478.

Rodger, C.J. (1999). Red sprites, upward lighting and VLF perturbations, Rev., Geophys., 37, 317-336.

Roeloffs, E.A. (1988). Hydrologic precursors to earthquakes: a review, Pure appl. Geophys., 126, 177-206.

Rozhnoi, A., M. Solovieva and M. Hayakawa (2013). VLF/LF signals method for searching of electromagnetic earthquake precursors, in Hayakawa M (eds), Earthquake Prediction Studies: Seismo Electromagnetics (pp 31-48), Terra Scientific Publishing, Tokyo.

Ryu, K., M. Parrot, S.G. Kim, K.S. Jeong, J.S. Chae, S. Pulinets and K. Oyama (2015). Suspected seismo-ionospheric coupling observed by satellite measurements and GPS TEC related to the M7.9 Wenchuan earthquake of 12 May 2008, J. Geophys. Res. Space Phys., 119, 10305-10323, http://doi.org/10.1002/2014JA020613.

Saito, A., T. Tsugawa, Y. Otsuka, M. Nishioka, T. Iyemori, M. Matsumura, et al. (2011). Acoustic resonance and plasma depletion detected by GPS total electron content observation after the 2011 off the Pacific coast of Tohoku earthquake, Earth Planets Space, 63, 863-867, https://doi.org/10.5047/eps.2011.06.034.

Scholz, C.H., L.R. Sykes and Y.P. Aggarwal (1973). Earthquake prediction: A physical basis, Science, 181, 803-809.

Scholz, C.H. (2002). The Mechanics of Earthquakes and Faulting, 2nd Edn., Cambridge University Press, Cambridge, UK.

Shen, X., H. Zhang, X. Yuan, S.G. Wang, L.W. Cao, J.B. Huang, J.P. Zhu, X.H. Piergiorgio and J.P. Dai (2018). The state-of-the-art of the China seismo-electromagnetic satellite mission, Sci. China Technol. Sci., 61, 634-642.

Shen, X., Q. Zong and X. Zhang (2018). Introduction to special section on the China seismo-electromagnetic satellite and initial results, Earth Planet. Phys., 2:439-443.

Shvets, A.V., M. Hayakawa, O.A. Molchanov and Y. Ando (2004). A study of ionospheric response to regional seismic activity by VLF radio sounding, Phys. Chem. Earth, 29, 627-637.

Sorokin, V., V. Chemyrev and M. Hayakawa (2015). Electrodynamic Coupling of Lithosphere-Atmosphere-Ionosphere of the Earth. Nova Science Publishing.

Sorokin, V., A.K. Yaschenko, V.M. Chmyrev and M. Hayakawa (2006). DC electric field amplification in the mid-latitude ionosphere over seismically active faults, Phys. Chem. Earth, 31, 447-453.

Su, X., G. Meng, H. Sun and W. Wu (2018). Positioning Performance of BDS Observation of the Crustal Movement Observation Network of China and Its Potential Application on Crustal Deformation, Sensors, 18, 3353, https://doi.org/10.3390/s18103353.

Sun, Y.-Y., C.-H. Chen, P. Zhang, S. Li, H. Xu, T. Yu, K. Lin, Z. Mao, D. Zhang, C.-Y. Lin and J.-Y. Liu (2022). Explosive eruption of the Tonga underwater volcano modulates the ionospheric E-region current on 15 January 2022, Geophys. Res. Lett., 49, e2022GL099621, doi:10.1029/2022GL099621.

Sun, Y.Y., J.Y. Lin, C.Y. Lin, H.F. Tasi, L.C. Chang, C.Y. Chen and C.H. Chen (2016). Ionospheric F2 region perturbed by the 25 April 2015 Nepal earthquake, J. Geophys. Res. Space Phys., 121, 5778-5784, http://doi.org/10.1002/2015JA022280.

Sun, Y.Y., K.I. Oyama, J.Y. Liu, H.K. Jhuang and C.Z. Cheng (2011). The neutral temperature in the ionospheric dynamo region and the ionospheric F region density during Wenchuan and Pingtung Doublet earthquakes, Nat. Hazards Earth Sys., 11, 1759-1768, http://doi.org/10.5194/nhess-11-1759-2011.

Sun, Y.-Y., T. Matsuo, E.A. Araujo-Pradere and J.Y. Liu (2013). Ground-based GPS observation of SED-associated irregularities over CONUS, J. Geophys. Res. Space Phys., 118, 2478-2489.

Takahashi, Y., R. Miyasato, T. Adachi, K. Adachi, M. Sera, A. Uchida and H. Fukunishi (2003). Activities of sprites and elves in the winter season, japan, J. Atmos. Sol.-Terr. Phys., 65(5), 551-560.

Tanimoto, T., S. Ishimaru and C. Alvizuri1 (2006). Seasonality in particle motion of microseisms, Geophys. J. Int., 166, 253-266.

Tramutoli, V., C. Aliano, R. Corrado, C. Filizzola, N. Genzano, M. Lisi, G. Martinelli and N. Pergola (2013). On the possible origin of thermal infrared radiation (TIR) anomalies in earthquake-prone areas observed using robust satellite techniques (RST), Chemical Geology, 339, 157-168.

Tramutoli, V., V. Cuomo, C. Filizzola, N. Pergola and C. Pietrapertosa (2005). Assessing the potential of thermal infrared satellite surveys for monitoring seismically active areas: The case of Kocaeli (Izmit) earthquake, 17 August 1999, Remote Sens. Environ., 96, 409-426.

Tronin, A.A. (1999). Satellite thermal survey application for earthquake prediction, in: Atmospheric and ionospheric phenomena associated with earthquakes, TERRAPUB, Tokyo, pp. 717-746, 1999.

Tsuda, T., Y. Murayama, T. Nakamura, R.A. Vincent, A.H. Manson, C.E. Meek and R.L. Wilson (1994). Variations of the gravity wave characteristics with height, season and latitude revealed by comparative observations, J. Atmos. Sol.-Terr. Phys., 56, 555-568.

Van Der Kamp, G., and J.E. Gale (1983). Theory of Earth tide and barometric effects in porous formations with compressible grains, Water Resour. Res., 19, 538-544.

VanZandt, T.E. (1985). A model for gravity wave spectra observed by Doppler sounding systems, Radio Sci., 20, 1323-1330.

Vidale, J., J. Mori and H. Houston (2001). Something wicked this way comes: Clues from foreshocks and earthquake nucleation, Eos Trans. AGU, 82, 68.

Wang, F., X. Zeng, L. Dong, J. Liu, Z. Mao, K. Lin and C.-H. Chen (2023). Monitoring seismo-TEC perturbations utilizing the Beidou geostationary satellites, Remote Sens., 15, 2608, https://doi.org/10.3390/rs15102608, 2023.

Xiao, Z., S.G. Xiao, Y.Q. Hao and D.H. Zhang (2007). Morphological features of ionospheric response to typhoon, J. Geophys. Res. Space Phys., 112, A04304, https://doi.org/10.1029/2006JA011671.

Xie, M., Y. Mang, G. Li, Z. Yuan, J. Zhong, S. Deng, J. Song, et al. (2021). Summary of Maduo MS 7.4 earthquake in Qinghai on May 22, 2021, Seismological and Geomagnetic Observation and Research, 42, 181-197, https://doi.org/10.3969/j.issn.1003-3246.2021.06.024. (in Chinese with English abstract)

Xu, G., W. Wan, C. She and L. Du (2008). The relationship between ionospheric total electron content (TEC) over East Asia and the tropospheric circulation around the Qinghai-Tibet Plateau obtained with a partial correlation method, Adv. Space Res., 42, 219-223.

Yamazaki, Y. and A. Maute (2016). Sq and EEJ—a review on the daily variation of the geomagnetic field caused by ionospheric dynamo currents, Space Sci. Rev., 206, 299-405.

Yang S.S. and M. Hayakawa (2020). Gravity wave activity in the stratosphere before the 2011 Tohoku earthquake as the mechanism of lithosphere-atmosphere-ionosphere coupling, Entropy, 22, 110.

Yasuoka, Y., G. Igarashi, T. Ishikawa, S. Tokonami and M. Shinogi (2006). Evidence of precursor phenomena in the Kobe earthquake obtained from atmospheric radon concentration, Appl. Geochem., 21, 1064-1072.

Zhang, Y. and Q. Meng (2019). A statistical analysis of TIR anomalies extracted by RSTs in relation to an earthquake in the Sichuan area using MODIS LST data, Nat. Hazards Earth Syst. Sci., 19, 535-549.

Zhao, J., Y. Geo, J. Tang, S.L. Klemperer, J. Wen., C.-H. Chen and J. Chong (2021). Electromagnetic Field Generated by an Earthquake Source Due to Motional Induction in 3D Stratified Media, and Application to 2008 *M*w 6.1 Qingchuan Earthquake, J. Geophys. Res., 126, e2021JB022102, https://doi.org/10.1029/2021JB022102.

Zhou, C., Y. Liu, S. Zhao, J. Liu, X. Zhang, J. Huang, X. Shen, B. Ni and Z. Zhao (2017). An electric field penetration model for seismo-ionospheric research, Adv. Space Res., 60(10), 2217-2232, https://doi.org/10.1016/j.asr.2017.08.007.

Zhuang, J., M. Matsu'ura, and P. Han (2021). Critical zone of the branching crack model for earthquakes: Inherent randomness, earthquake predictability, and precursor modeling, The European Physical Journal Special Topics, 230, 409-424, https://doi.org/10.1140/epjst/e2020-000272-7.

***CORRESPONDING AUTHOR: Chieh-Hung CHEN**,
Institute of Geophysics and Geomatics, China University of Geosciences, Wuhan, Hubei, 430074, China
e-mail: nononochchen@gmail.com